Received May 18, 2019, accepted June 13, 2019, date of publication June 19, 2019, date of current version July 8, 2019.

Digital Object Identifier 10.1109/ACCESS.2019.2923584

Nondata-Aided Error Vector Magnitude Analysis of $\eta - \mu$ Fading Channels in Device-to-Device Communications

FAN YANG[1], HAIWEI MAO[2], XIAOPING ZENG[2], XIN JIAN[2], SHU FU[2], BIN WU[3], (Member, IEEE), XIAOHENG TAN[2], AND JIHUA ZHOU[4]

[1]School of Electrical and Electronic Engineering, Chongqing University of Technology, Chongqing 400054, China
[2]College of Communication Engineering, Chongqing University, Chongqing 400044, China
[3]School of Computer Science and Technology, Tianjin University, Tianjin 300072, China
[4]Chongqing Jinmei Communication Company Ltd., Chongqing 400030, China

Corresponding author: Haiwei Mao (34179861@qq.com)

This work was supported in part by the National Natural Science Foundation of China under Grant 61501065, Grant 61601067, Grant 61571069, and Grant 91438104, in part by the Scientific Research Foundation of Chongqing University of Technology, and in part by the Chongqing Research Program of Basic Research and Frontier Technology under Grant CSTC2016JCYJA0021.

ABSTRACT Transmission in non-line-of-sight (NLOS) conditions has a poor throughput in device-to-device (D2D) communications. In order to achieve high throughput, adaptive modulation has been selected as a spectrally-efficient transmission technology. Moreover, quantifying the performance of a fading channel in NLOS conditions becomes a core issue. In general, the $\eta - \mu$ distribution can be employed to characterize and model the NLOS fading channel. Effective evaluating the quality of $\eta - \mu$ channels can provide an efficient theoretical reference for determining the optimum switching thresholds in adaptive modulation. However, due to the sensitivity of D2D transmission to fading channels, providing an efficient theoretical benchmark for evaluating, the quality of $\eta - \mu$ channels is still a challenge in transmission design. In this paper, the nondata-aided error vector magnitude (NDA-EVM) is considered as a novel metric to evaluate the quality of wireless fading channels. Specifically, the NDA-EVM of the multilevel quadrature amplitude modulation (MQAM) signals over $\eta-\mu$ fading channels and its lower bound is analytically derived. This can be used to further determine the optimum switching thresholds in adaptive modulation in NLOS conditions. The numerical results validate the effectiveness of the proposed formulation and also reveal the influence of the channel parameters on the lower bound of the NDA-EVM.

INDEX TERMS $\eta - \mu$ fading channels, D2D, NLOS, nondata-aided error vector magnitude, lower bound.

I. INTRODUCTION

Device-to-device (D2D) communication is one of the key techniques in the 5th generation (5G) wireless communication systems that allows direct communication between mobile nodes [1]. However, D2D transmission schemes are sensitive to channel conditions and provide poor throughput in Non-line-of sight (NLOS) scenarios [2]. Adaptive modulation can select the optimal modulation parameters relative to the channel characteristics, which can provide an effective leverage to achieve high throughput [3]. Hence, quantifying the performance of a fading channel in NLOS conditions is a core issue of adaptive modulation in D2D communications.

The associate editor coordinating the review of this manuscript and approving it for publication was Rui Wang.

The $\eta - \mu$ distribution is a general fading distribution that represents inhomogeneous, non-circularly symmetric channel environments, which can fit well for NLOS conditions in D2D communications [4]–[6]. Many well-known distributions (e.g., the Nakagami-q, Hoyt, Nakagami-m, and Rayleigh distributions) are special cases of the $\eta - \mu$ distribution [4], [7]. Since the evaluation of $\eta - \mu$ fading channels can provide a theoretical basis for determining the optimum switching thresholds in adaptive modulation, how to quantify $\eta-\mu$ channels has attracted extensive attentions and becomes a research focus. Traditionally, classic metric such as the bit error ratio (BER) and the signal-to-noise ratio (SNR) is used to quantify the performance of a fading channel [8], [9]. However, the calculation of BER requires long-term statistical computations, and SNR estimation requires many

known data sequences (e.g., preambles an d pilots). When the communication over rapidly time-varying channels, the traditional estimations will make a non-real-time error because of the fixed time interval between these known data sequences [10]. Moreover, the D2D transmission is sensitive to fading channels. Using traditional metric for adaptive modulation over $\eta-\mu$ channels in D2D communications is inappropriate. Hence, providing an efficient theoretical benchmark for evaluating the quality of $\eta-\mu$ channels is still a challenge, and becomes a bottleneck for D2D transmission design.

This paper proposes the nondata-aided error vector magnitude (NDA-EVM) as a new performance metric for evaluating the quality of the generalized $\eta-\mu$ channels. NDA-EVM reflects the error between the received symbol and the transmitted symbol [10], [11].

Unlike using the data-aided SNR (DA-SNR) or EVM to evaluate the quality of channel, which update the measurements in a periodic manner (update period is affected by the fixed time interval between the aided data), NDA-EVM can quantify and update the measurements only by a few received symbols. The characteristic of NDA-EVM shows that it is sensitive to the degradation of fading channels, which is important for real-time tracking channel changes. Even when the packet reception fails, some achievable system performance (e.g., the symbol error rate (SER), throughput and outage probability) can also be inferred by NDA-EVM [10], [12]. Thus, it is preferable to use NDA-EVM to characterize system performance in D2D communications. In contrast to the abundance of traditional SNR and BER performance analyses of the generalized $\eta-\mu$ fading channels, few studies have quantified the achievable NDA-EVM performances in $\eta-\mu$ fading channels. Although the authors of [13] presented a theoretical formulation for the data-aided EVM over $\eta-\mu$ channels using SNR as an intermediate variable, there is no simple correspondence between NDA-EVM and SNR, moreover, the relationship between NDA-EVM and the $\eta-\mu$ distribution remains an open problem. Motivated by these observations, the theoretical NDA-EVM performance analysis of signals transmitted over $\eta-\mu$ fading channels has become a core issue in D2D communications. In this paper, we relate NDA-EVM to $\eta-\mu$ fading channels using the fading channel gain as an intermediate variable, and present the close-form expression of NDA-EVM. By applying inequalities properties and properly zooming to the close-form expression, we obtain the theoretical bound for NDA-EVM over $\eta-\mu$ fading channels in D2D.

There are four primary contributions in this paper:

1) NDA-EVM is employed to analyze $\eta-\mu$ fading channels in D2D;

2) A closed-form expression for NDA-EVM of multilevel quadrature amplitude modulation (MQAM) signals over fading channels is derived;

3) A lower bound on NDA-EVM for $\eta-\mu$ fading channels is formulated based on this closed-form expression;

4) The influences that are exerted on the lower bound by parameters such as η, μ and the signal modulation order are studied.

Various performance evaluation results obtained through analysis and simulations confirm that the derived lower bound is close to the theoretical value in the region of low μ and high η. The lower bound is sensitive to the variation of the channel parameters, especially the parameter μ. The results of this study can also serve as a reference for determining the optimum switching thresholds in adaptive modulation in D2D communications.

II. THE $\eta-\mu$ FADING CHANNEL MODEL

For a single-input single-output (SISO) system in D2D communications, MQAM signals received over $\eta-\mu$ fading channels are modeled as follows:

$$y=\alpha x+w, \tag{1}$$

where w is an i.i.d. complex Gaussian noise with zero mean and variance σ_n^2. Given the normalized fading channel gain α ($0<\alpha<1$), the probability density function (PDF) of the fading power ($z=\alpha^2$) in $\eta-\mu$ channels is derived in (2) using the PDF of the sum of two gamma random variables in a SISO system [14]:

$$f_{Z,\eta-\mu}(z)=\frac{z^{2\mu-1}}{\theta_1^{\mu}\theta_2^{\mu}\Gamma(2\mu)}\Phi_2^{(2)}(\mu,\mu;2\mu;\frac{-z}{\theta_1},\frac{-z}{\theta_2}), \tag{2}$$

where $\Phi_2^{(2)}(\cdot)$ is the confluent Lauricella function [15]. The gamma RVs have the same shape parameter μ but different scale parameters of the forms $\theta_1=\frac{E(z)}{2\mu(h+H)}$ and $\theta_2=\frac{E(z)}{2\mu(h-H)}$, where $h=\frac{2+\eta^{-1}+\eta}{4}$, $H=\frac{\eta^{-1}-\eta}{4}$ in Format 1 and $h=\frac{1}{1-\eta^2}$, $H=\frac{\eta}{1-\eta^2}$ in Format 2; and $X=\alpha^2$, $\mu=\frac{E^2\{X\}}{2var\{X\}}[1+(\frac{H}{h})^2]$.

Considering $z=\alpha^2$, the PDF of α is given by

$$f_{\alpha,\eta-\mu}(\alpha)=\frac{2\alpha^{4\mu-1}}{\theta_1^{\mu}\theta_2^{\mu}\Gamma(2\mu)}\Phi_2^{(2)}(\mu,\mu;2\mu;\frac{-\alpha^2}{\theta_1},\frac{-\alpha^2}{\theta_2}) \tag{3}$$

III. NDA-EVM OF MQAM SIGNALS

NDA-EVM is defined as the root mean square (RMS) value of the difference between the received symbols y and the estimated transmitted symbols $\hat{x}$ [11]. It can be shown that

$$\xi[M]=\sqrt{\sum_{n=1}^{N}\left|y[n]-\hat{x}[n]\right|^2/NP_0}, \tag{4}$$

Remarkably, the n^{th} estimated transmitted symbol $\hat{x}[n]$ can be obtained from the received symbols $y[n]$ by means of maximum likelihood (ML) estimation. P_0 is the normalized received symbol power, $P_0=1$. For simplicity, the index n is dropped for the remainder of this discussion. Suppose that x is an MQAM signal of modulation order M; then,

$x \in \{S_1, \ldots, S_i, \ldots, S_M\}$, where S_i is the i^{th} constellation point in the constellation set and can be expressed as [2]

$$\begin{aligned} S_i &= S_{i,R} + jS_{i,I} = (2i-k)b + j(2m-k)b, \\ i, m &= 0, 1, \cdots k; \quad b = \sqrt{3/2(M-1)}; \ \& \ k = \sqrt{M} - 1. \end{aligned} \tag{5}$$

In (5), b is the normalized symbol amplitude. Because the real and imaginary parts of MQAM signals are independent and symmetrical, only the real part is considered in the following. So, (4) can be simplified as

$$\begin{aligned} \xi[M]^2 &= 2E\{(y_R - \hat{x}_R)^2\} \\ &= 2\sum_{i=0}^{k} P(\hat{x}_R = S_{i,R}) \\ &\quad \times \int_{-\infty}^{+\infty} (y_R - S_{i,R})^2 f(y_R|\hat{x}_R = S_{i,R}) dy_R. \end{aligned} \tag{6}$$

From (1), the conditional PDF of the received symbol y_R is

$$f(y_R|x_R = S_{i,R}) = \frac{1}{\sigma_n}\varphi(\frac{y_R - \alpha S_{i,R}}{\sigma_n}), \tag{7}$$

where $\varphi(\cdot)$ is the probability density function of the standard normal distribution.

Using total probability theorem [16], the probability of $\hat{x}_R = S_{i,R}$ is

$$P(\hat{x}_R = S_{i,R}) = \sum_{j=0}^{k} P(x_R = S_{j,R}) \int_{D_{i,R}} f(y_R|x_R = S_{j,R}) dy_R, \tag{8}$$

where $D_{i,R}$ is the decision region for symbol $S_{i,R}$, and can be confirmed by the ML criterion:

$$D_{i,R} = \begin{cases} -\infty < y_R \le S_{0,R} + b, & if \ i = 0; \\ S_{i,R} - b < y_R \le S_{i,R} + b & if \ 1 \le i \le k-1; \\ S_{k,R} - b < y_R < \infty & if \ i = k. \end{cases} \tag{9}$$

It is assumed that the probability of transmitted symbol is $P(x_R = S_{j,R}) = 1/(1+k), \forall j$. By the definition of conditional probability, $f(y_R|\hat{x}_R = S_{i,R})$ can be evaluated as follows:

$$f(y_R|\hat{x}_R = S_{i,R}) = \frac{f(\hat{x}_R = S_{i,R}|y_R) f(y_R)}{f(\hat{x}_R = S_{i,R})}, \tag{10}$$

When $y_R \in D_{i,R}, f(\hat{x}_R = S_{i,R}|y_R) = 1$; and for all other y_R, $f(\hat{x}_R = S_{i,R}|y_R) = 0$. Hence, (10) can be rewritten as:

$$f(y_R|\hat{x}_R = S_{i,R}) = \frac{f(y_R)}{f(\hat{x}_R = S_{i,R})}, \quad y_R \in D_{i,R} \tag{11}$$

According to the total probability theorem:

$$f(y_R|\hat{x}_R = S_{i,R}) = \frac{\sum_{j=0}^{k} f(y_R|x_R = S_{j,R})}{\sum_{j=0}^{k} \int_{D_{i,R}} f(y_R|x_R = S_{j,R}) dy_R}, \quad y_R \in D_{i,R} \tag{12}$$

By using (8) and (12), and after some derivations, (6) can be reduced to (13), as shown at the bottom of this page. (the derivation is in the Appendix A).

Where $\lambda_{ji,R} = -S_{i,R} + \alpha S_{j,R}$ and $Q(\cdot)$ is a complementary cumulative distribution function (CCDF).

By simplifying (13) (as shown in the Appendix B), the NDA-EVM of the MQAM signals can be lower bounded in (14):

$$\xi[M] > \frac{\sigma_n + bk}{(2\pi)^{1/4}} \exp(-\frac{b^2[(1+k)^2 + 2k(1+k)] + b^2k^2\alpha^2}{4\sigma_n^2}). \tag{14}$$

IV. LOWER BOUND FOR $\eta-\mu$ CHANNELS

NDA-EVM of signals transmitted over an $\eta-\mu$ fading channel is given by [11].

$$NDA - EVM_{\eta-\mu} = \int_0^1 \xi[M] f_{\alpha,\eta-\mu}(\alpha) d\alpha, \tag{15}$$

which is an $\eta-\mu$ fading channel's NDA-EVM and can be evaluated by integrating over the range of all possible α values. The lower bound on NDA-EVM for an $\eta-\mu$ channel can then be obtained by substituting (3) and (14) into (15) and setting $t = b^2k^2\alpha^2/4\sigma_n^2$. It can be rewritten as

$$\begin{aligned} NDA - EVM_{\eta-\mu} > \int_0^{\infty} &\frac{\tau(k) e^{-t}}{\theta_1^{\mu}\theta_2^{\mu}\Gamma(2\mu)} \beta(k)^{2\mu} t^{2\mu-1} \\ &\times \Phi_2^{(2)}(\mu, \mu; 2\mu; \frac{-\beta(k)t}{\theta_1}, \frac{-\beta(k)t}{\theta_2}) dt, \end{aligned} \tag{16}$$

$$\begin{aligned} \xi[M]^2 = 2/(k+1)\{&\sum_{j=0}^{k} [\sigma_n(-b + \lambda_{jk,R})\varphi(\frac{-b-\lambda_{jk,R}}{\sigma_n}) + (\lambda_{jk,R}^2 + \sigma_n^2) Q(\frac{-b-\lambda_{jk,R}}{\sigma_n})] + \sum_{j=0}^{k} [\sigma_n(b + \lambda_{jk,R})\varphi(\frac{b-\lambda_{jk,R}}{\sigma_n}) \\ &+ (\lambda_{jk,R}^2 + \sigma_n^2) Q(\frac{b-\lambda_{jk,R}}{\sigma_n})] + \sum_{i=1}^{k}\sum_{j=0}^{k} [\sigma_n(-b + \lambda_{ji,R})\varphi(\frac{-b-\lambda_{ji,R}}{\sigma_n}) + (\lambda_{ji,R}^2 + \sigma_n^2) Q(\frac{-b-\lambda_{ji,R}}{\sigma_n})] \\ &- \sum_{i=1}^{k}\sum_{j=0}^{k} [\sigma_n(b + \lambda_{ji,R})\varphi(\frac{b-\lambda_{ji,R}}{\sigma_n}) + (\lambda_{ji,R}^2 + \sigma_n^2) Q(\frac{b-\lambda_{ji,R}}{\sigma_n})]\} \end{aligned} \tag{13}$$

TABLE 1. Table of special cases.

Special case	NDA-EVM Lower bound	Parameter settings
Nakagami-m	$\frac{1}{k^{2p^*}}\frac{\Gamma(m-p^*)}{m^m\Gamma(m)}\tau(k)\beta(k)^{m-p^*}\,{}_2F_1[m-p^*,m,m;-m\beta(k)]$	η=1, $\mu=m/2$
Nakagami-q	$\frac{\tau(k)\beta(k)^{1-p^*}}{k^{2p^*}}(\frac{1+q}{2q})\frac{\Gamma(1-p^*)}{\Gamma(1)}F_D^{(2)}(1-p^*,0.5,0.5;1;-(\frac{1}{2q^2}+\frac{1}{2})\beta(k),-(\frac{1}{2}+\frac{q^2}{2})\beta(k))$	$\eta=q^2$, $\mu=0.5$
Rayleigh	$\frac{1}{k^{2p^*}}\frac{\Gamma(p^*)}{\Gamma(1)}\tau(k)\beta(k)^{1-p^*}\,{}_2F_1[1-p^*,1;1;-\beta(k)]$	η=1, $\mu=0.5$

where $\tau(k)=\frac{\sigma_n+bk}{(2\pi)^{1/4}}\exp(-\frac{b^2[(1+k)^2+2k(1+k)]}{4\sigma_n^2})$ and $\beta(k)=\frac{4\sigma_n^2}{b^2k^2}$. Without loss of generality, p is introduced[1] ($p>0$), and (16) is transformed into (17):

$$NDA-EVM_{\eta-\mu} > \int_0^\infty \frac{\tau(k)e^{-t}}{\theta_1^\mu\theta_2^\mu\Gamma(2\mu)}\beta(k)^{2\mu-p}\frac{1}{k^{2p}}(\frac{2\sigma_n}{b})^{2p} \times t^{2\mu-1-p}t^p\Phi_2^{(2)}(\mu,\mu;2\mu;\frac{-\beta(k)t}{\theta_1},\frac{-\beta(k)t}{\theta_2})dt. \quad (17)$$

When $\alpha\geq 1/k$ and $t^p(2\sigma_n/b)^{2p}=(k\alpha)^{2p}\geq 1$, (17) can be rewritten as

$$NDA-EVM_{\eta-\mu} > \int_0^\infty \frac{1}{k^{2p}}\tau(k)\beta(k)^{2\mu-p}\exp(-t) \times \frac{t^{2\mu-p-1}}{\theta_1^\mu\theta_2^\mu\Gamma(2\mu)}\Phi_2^{(2)}(\mu,\mu;2\mu;\frac{-\beta(k)t}{\theta_1},\frac{-\beta(k)t}{\theta_2})dt. \quad (18)$$

According to the property of Lauricella's function of the fourth kind $F_D^{(n)}[\cdot]$ [15]

$$F_D^{(n)}[a,b_1,\cdots,b_n,c,x_1,\cdots,x_n] = \frac{1}{\Gamma(a)}\int_{t=0}^\infty e^{-t}t^{a-1}\Phi_2^{(n)}(b_1,\cdots,b_n,c,x_1t,\cdots,x_nt)dt, \quad (19)$$

(18) is equivalent to

$$NDA-EVM_{\eta-\mu} > \frac{1}{k^{2p}}\tau(k)\beta(k)^{2\mu-p}\frac{\Gamma(2\mu-p)}{\theta_1^\mu\theta_2^\mu\Gamma(2\mu)} \times F_D^{(2)}(2\mu-p,\mu,\mu;2\mu;\frac{-\beta(k)}{\theta_1},\frac{-\beta(k)}{\theta_2}). \quad (20)$$

In (20), the optimal $p=p^*$ can be searched,

$$p^*=\arg\max_{p\in(0,2\mu)}\{\frac{\beta(k)^{2\mu-p}}{k^{2p}}\frac{\Gamma(2\mu-p)}{\theta_1^\mu\theta_2^\mu\Gamma(2\mu)} \times F_D^{(2)}(2\mu-p,\mu,\mu;2\mu;\frac{-\beta(k)}{\theta_1},\frac{-\beta(k)}{\theta_2})\}, \quad (21)$$

[1]The constraint of (19) is Real(c) > Real(a) > 0; p is used to guarantee that (16) satisfies this constraint.

where $p\in(0,2\mu)$. We simplify (20) for several special cases as shown in Table 1.

V. PARAMETRIC ANALYSIS OF THE LOWER BOUND

To validate the lower bound on NDA-EVM derived for $\eta-\mu$ fading channels with arbitrary parameters, the Monte Carlo approach is utilized to simulate MQAM signals transmitted over $\eta-\mu$ channels. By implementing a simulation-based solution of (15), theoretical NDA-EVM values are obtained. To compare performance results under the same conditions, we use 1 transmit antenna and 1 receive antenna and set the average symbol power of the MQAM signals to 1 watt in the simulations.

A. VARIATION OF NDA-EVM LOWER BOUND WITH η AND μ

Fig. 1 shows NDA-EVM lower bounds for QAM signals transmitted over $\eta-\mu$ fading channels. It can be seen that the lower bound is affected by the channel parameters μ and η for a fixed modulation order. The two channel parameters exert different influences on the lower bound. An increase in μ results in a smaller lower bound on NDA-EVM, and when μ is sufficiently large (e.g., $\mu>8$), the lower bound converges. By contrast, an increase in the parameter η results in an increase in the lower bound, which also converges when η is sufficiently large (e.g., $\eta>18$).

B. NDA-EVM PERFORMANCE FOR DIFFERENT MODULATION ORDER OF MQAM

Fig. 2 shows the lower bounds on NDA-EVM for different modulation orders, with $\eta=1$ and $\mu=0.5$ in Format 1 (a Rayleigh fading channel). By means of a numerical search, the optimal p^* values for the lower bound in (21) are confirmed (i.e., for QAM, $p^*=0.21$; for 16QAM, $p^*=0.84$; and for 64QAM, $p^*=0.99$). The results show that the lower bound on NDA-EVM is a decreasing function of M (i.e., $M=k^2+1$). This property is revealed by (16), which shows that NDA-EVM lower bound is mainly a function of e^{-k^2}. Compared with that in the high-SNR region, the gap between the theoretical result and the lower bound is smaller in the low-SNR region.

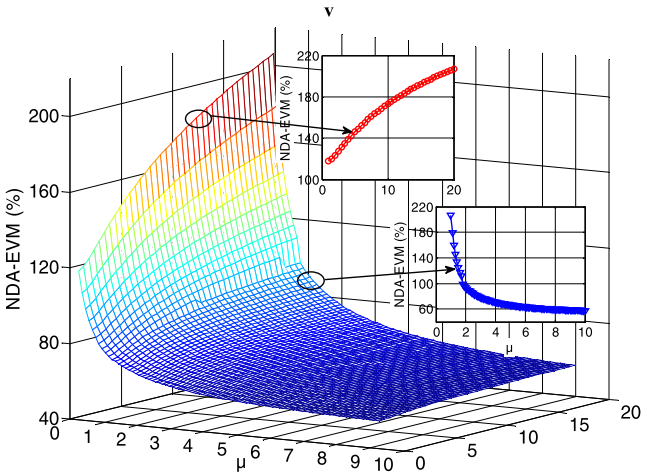

FIGURE 1. Variation of NDA-EVM lower bound with the parameters η and μ (QAM signals).

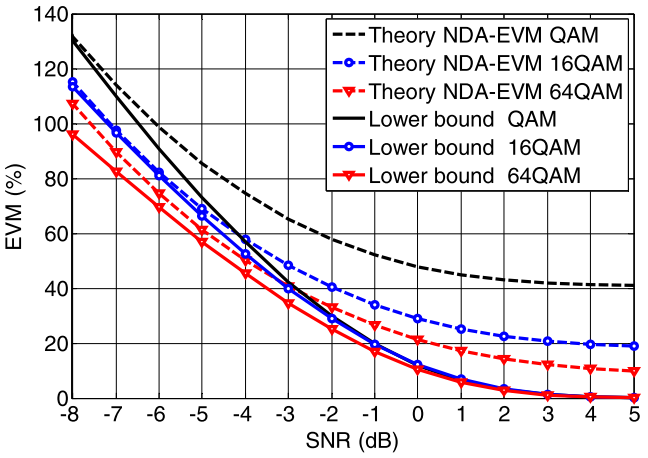

FIGURE 2. NDA-EVM performance for different modulation order of MQAM.

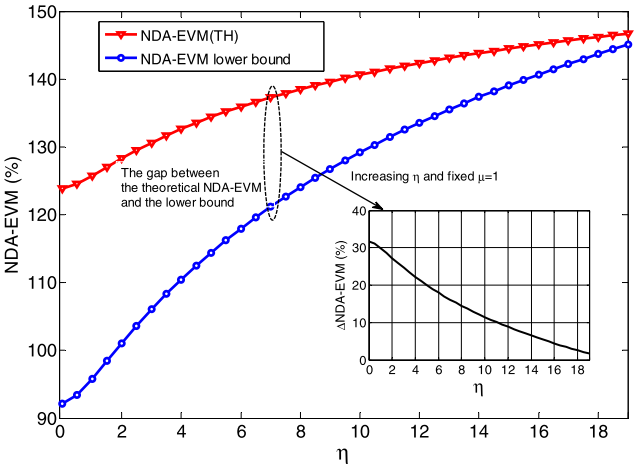

FIGURE 3. NDA-EVM results for different values of η with a fixed value of $\mu = 1$ (QAM signals).

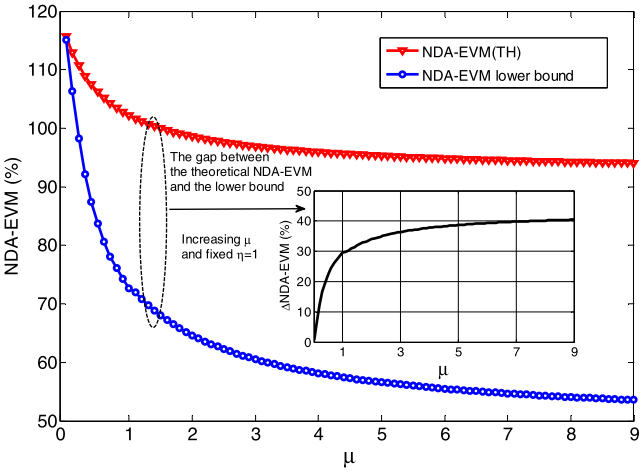

FIGURE 4. NDA-EVM results for different values of μ with a fixed value of $\eta = 1$ (QAM signals).

C. INFLUENCE OF THE PARAMETER η ON THE LOWER BOUND

Fig. 3 compares the lower bound with the theoretical NDA-EVM values for QAM signals transmitted over $\eta - \mu$ channels of Format 1 where $\mu = 1$ and η is arbitrary. It is obviously that the lower bound is an increasing function of η for a fixed μ. Because η is the power ratio of the in-phase and quadrature-phase components of the fading signal [4], increment in η implies increasingly severe fading of the QAM signal, and the lower bound increases accordingly. Remarkably, the lower bound converges to the theoretical NDA-EVM with increasing η. In other words, the lower bound is fairly closed to the theoretical value in the high η region.

D. INFLUENCE OF THE PARAMETER μ ON THE LOWER BOUND

Fig. 4 shows the lower bound and the theoretical NDA-EVM values of QAM signals for various values of μ with a fixed value of $\eta = 1$. μ has the opposite effect on the lower bound as that of η; the lower bound is a decreasing function of μ for a fixed η. As μ increases, the gap between the lower bound and the theoretical NDA-EVM initially increases and then converges to a constant value (e.g., Δ NDA-EVM $\rightarrow$ 40% when $\mu > 7$). However, the lower bound is close to the theoretical value in the low μ region. In addition, from a comparison of the variations in the lower bound caused by variations in the parameters η and μ as depicted in Fig. 3 and Fig. 4, it is evident that the lower bound is more sensitive to μ. Consequently, a slight variation in μ leads to a greater variation in the lower bound.

VI. PERFORMANCE EVALUATION

Performance evaluations of adaptive modulation over $\eta - \mu$ fading channels can provide useful guidance for D2D transmission design. 1) Accuracy of the channel quality metric and 2) outage capacity are two most important performance evaluation parameters in the system. To justify the effectiveness of applying the present work in adaptive modulation, we simulate adaptive modulation system that uses

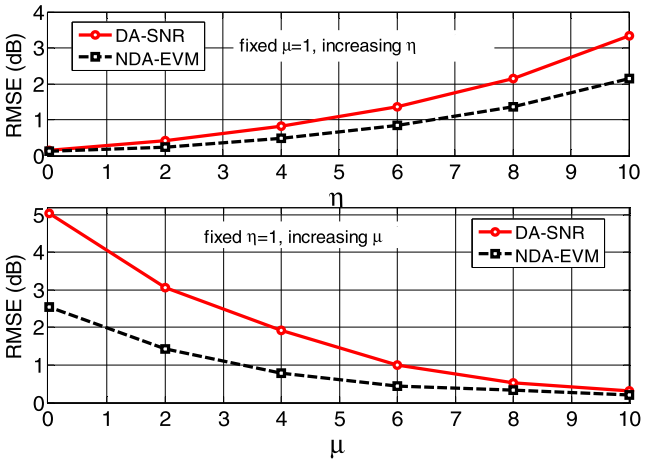

FIGURE 5. The RMSE of the estimated channel quality metric for an $\eta - \mu$ fading channel.

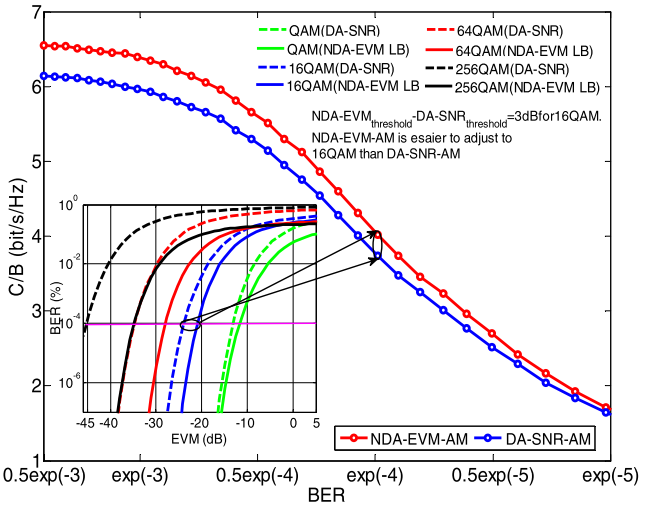

FIGURE 6. Outage capacity comparison between NDA-EVM-AM and DA-SNR-AM.

MQAM (including QAM, 16QAM, 64QAM and 256QAM). The simulated channel model is the $\eta - \mu$ fading channel, and the data frame format is reference to Physical Uplink Shared Channel (PUSCH) specified in the 3GPP LTE-Hi standard [10], [17].

A. ACCURACY OF THE CHANNEL QUALITY METRIC

The root mean square error (RMSE) as a statistical parameter is used to evaluate the deviations between estimated and real value, so RMSE is considered as the standard for measuring the accuracy of the channel quality metric. We compare the estimation of NDA-EVM with the traditional DA-SNR metric (e.g., there is 1 reference signal (RS) every 7 data symbols in the PUSCH for normal cyclic prefix (CP), and RS is the aided data using for SNR estimation) over $\eta - \mu$ channels.

We simulate the MQAM signals transmitted over the $\eta - \mu$ fading channels with different μ and η, and estimated NDA-EVM (i.e., ξ_E) by using (13) for every $\eta - \mu$ fading channel. To obtain real NDA-EVM (i.e., ξ_R), we use Monte Carlo approach (i.e., $n = 1000$ rounds in our simulation) to compare the deviation between the received constellation and the ideal constellation point. The RMSE of NDA-EVM can be obtained as $RMSE = \sqrt{\sum (\xi_R - \xi_E)^2 / n}$. In a similar way, the RMSE of DA-SNR can also be obtained.

As the channel parameter μ increases, the channel changes slowly [18]. It also makes the estimation of channel quality becomes more accuracy, so the RMSE decreases, as shown in Fig. 5. Because the fixed update frequency of the channel quality estimation can't trace the channel variation effectively, the data-aided estimation accuracy is more affected by the variations in μ. By contrast, NDA-EVM estimation is more robust and its RMSE is lower than DA-SNR. As analyzed in Section V, η has the opposite effect on the lower bound from that of μ, the RMSE increases with η. The same analysis showed the NDA-EVM estimation has lower RMSE than DA-SNR. As a metric to evaluate the quality of wireless fading channels, NDA-EVM is more effective than DA-SNR.

B. OUTAGE CAPACITY

The outage capacity of an adaptive modulation system can be defined as the maximum data rate while maintaining a certain outage probability over a fading channel [19]. The result reflects the upper bound of the performance in a realistic system. We compare the outage capacity for NDA-EVM-based adaptive modulation (NDA-EVM-AM) with that for the traditional SNR-based adaptive modulation (DA-SNR-AM) reported in [20] when $P_{out} = 0.1$. We adopt a fading channel scenario with parameter values of $\eta = 1$ and $\mu = 0.5$ in Format 1 (i.e., a Rayleigh fading channel).

While achieving the expected SER such that the P_{out} limit is satisfied, NDA-EVM-AM algorithm chooses the highest modulation order that can tolerate the lower bound on NDA-EVM at the receiver. Fig. 6 shows that for the target SER, the switching threshold based on NDA-EVM is higher[2] than that of DA-SNR at the same modulation order, which means the switching threshold of NDA-EVM is easier to achieve. For example, the 16QAM switching threshold for NDA-EVM is 3 dB higher than DA-SNR (which can be translated into EVM using the formula $EVM = \sqrt{1/SNR}$ [21]). For the same modulation order, bigger NDA-EVM indicates poorer channel quality. Thus NDA-EVM-AM can be used to transmit 16QAM signals under the target P_{out} under a poor channel condition, whereas DA-SNR-AM must remain QAM modulation order. Consequently, NDA-EVM-AM has a higher outage capacity, and this analysis also proves that the lower bound on NDA-EVM is useful for determining the optimum switching thresholds in adaptive modulation over $\eta - \mu$ channels.

[2]discussion of the relationship between NDA-EVM or DA-SNR and the SER for $\eta - \mu$ an fading channel is outside the scope of this article, we obtained the curves through Monte Carlo simulations.

VII. CONCLUSION

In this paper, NDA-EVM was proposed as a performance metric for wireless fading channels, and an analytical procedure was developed to investigate NDA-EVM for the generalized $\eta-\mu$ fading channels. A lower bound on NDA-EVM was derived for MQAM signals transmitted over $\eta-\mu$ fading channels, and this lower bound was simplified for various special cases. A parametric study of the lower bound was also presented. Simulation results showed that the lower bound, which depends on the modulation order M and the values of the parameters η and μ, is close to the theoretical value in the region of low μ and high η. In particular, the channel parameter μ exerts a more significant impact on the lower bound. Since the derived lower bound serves as an effective benchmark for channel quality, this study provides a reference for determining the optimum switching thresholds in adaptive modulation of D2D communications.

APPENDIX A

Because every modulation constellation point in MQAM is transmitted with equal probability. So, $P(x_R = S_{j,R}) = 1/(1+k)$, $\forall j$. From (8) and (12), the expression in (6) is reduced to

$$\begin{aligned}\xi[M]^2 &= 2E\{(y_R-\hat{x}_R)^2\}\\ &= \frac{2}{k+1}\sum_{i=0}^{k}\sum_{j=0}^{k}\int_{D_{i,R}}(y_R-S_{i,R})^2\frac{1}{\sigma_n}\varphi(\frac{y_R-\alpha S_{j,R}}{\sigma_n})dy_R\end{aligned} \tag{22}$$

By using $v = y_R - S_{i,R}$, $\tilde{D}_{i,R} = D_{i,R} - S_{i,R}$, and letting $\lambda_{ji,R} = -S_{i,R} + \alpha S_{j,R}$, (22) is simplified to

$$\xi[M]^2 = \frac{2}{k+1}\sum_{i=0}^{k}\sum_{j=0}^{k}\int_{\tilde{D}_{i,R}}\frac{v^2}{\sigma_n}\varphi(\frac{v-\lambda_{ji,R}}{\sigma_n})dv. \tag{23}$$

The integral in (23) can be divided into two parts, the first part is the decision regions of $\tilde{D}_{i,R}$ with $i = 0, k$, and the second part is $\tilde{D}_{i,R}$ with $1 \le i \le k-1$. So (23) can be rewritten as

$$\begin{aligned}\xi[M]^2 = \frac{2}{k+1}\sum_{i=0}^{k}\sum_{j=0}^{k}[&\int_{-\infty}^{b}\frac{v^2}{\sigma_n}\varphi(\frac{v-\lambda_{j0,R}}{\sigma_n})dv\\ &+\int_{-b}^{b}\frac{v^2}{\sigma_n}\varphi(\frac{v-\lambda_{ji,R}}{\sigma_n})dv+\int_{-b}^{\infty}\frac{v^2}{\sigma_n}\varphi(\frac{v-\lambda_{jk,R}}{\sigma_n})dv].\end{aligned} \tag{24}$$

Considering $\varphi(x) = \varphi(-x)$ and $\lambda_{j0,R} = -\lambda_{jk,R}$

$$\sum_{j=0}^{k}\int_{-\infty}^{b}\frac{v^2}{\sigma_n}\varphi(\frac{v-\lambda_{j0,R}}{\sigma_n})dv = \sum_{j=0}^{k}\int_{-b}^{\infty}\frac{v^2}{\sigma_n}\varphi(\frac{v-\lambda_{jk,R}}{\sigma_n})dv, \tag{25}$$

and define Z-function as

$$z(x,\lambda,\sigma) = \frac{1}{\sigma}\int_{x}^{\infty}v^2\varphi(\frac{v-\lambda}{\sigma})dv. \tag{26}$$

(24) can be rewritten as

$$\begin{aligned}\xi[M]^2 &= \frac{2}{k+1}(2\sum_{j=0}^{k}z(-b,\lambda_{jk,R},\sigma_n)\\ &\quad+\sum_{i=1}^{k-1}\sum_{j=0}^{k}[z(-b,\lambda_{ji,R},\sigma_n)-z(b,\lambda_{ji,R},\sigma_n)])\\ &= \frac{2}{k+1}[\sum_{j=0}^{k}z(-b,\lambda_{jkR},\sigma_n)+\sum_{j=0}^{k}z(b,\lambda_{jkR},\sigma_n)\\ &\quad+\sum_{i=1}^{k}\sum_{j=0}^{k}z(-b,\lambda_{ji,R},\sigma_n)-\sum_{i=1}^{k}\sum_{j=0}^{k}z(b,\lambda_{ji,R},\sigma_n)].\end{aligned} \tag{27}$$

By using the property of Z-function [21]

$$z(x,\lambda,\sigma) = \sigma(x+\lambda)\varphi(\frac{x-\lambda}{\sigma})+(\lambda^2+\sigma^2)Q(\frac{x-\lambda}{\sigma}). \tag{28}$$

NDA-EVM can be reduced to (13).

APPENDIX B

It can be seen from (13), NDA-EVM is a sum of the errors over two kinds of decision regions. (i.e., singly truncated decision regions $D_{0,R}$, $D_{k,R}$, and doubly truncated decision regions $D_{i,R}$). Because the summation in $D_{i,R}$ is much smaller than that in $D_{0,R}$ and $D_{k,R}$, and it is always positive. (13) can be simplified to

$$\begin{aligned}\xi[M]^2 > \frac{2}{k+1}\{&\sum_{j=0}^{k}[\sigma_n(-b+\lambda_{jk,R})\varphi(\frac{-b-\lambda_{jk,R}}{\sigma_n})\\ &+(\lambda_{jk,R}^2+\sigma_n^2)Q(\frac{-b-\lambda_{jk,R}}{\sigma_n})]+\sum_{j=0}^{k}[\sigma_n(b+\lambda_{jk,R})\\ &\times\varphi(\frac{b-\lambda_{jk,R}}{\sigma_n})+(\lambda_{jk,R}^2+\sigma_n^2)Q(\frac{b-\lambda_{jk,R}}{\sigma_n})]\}.\end{aligned} \tag{29}$$

Since

$$\lambda_{jk,R} = b[\alpha(j-k)+(\alpha j-k)] < 0, \tag{30}$$

and $Q(x)$ decreases monotonically, we can get

$$Q(\frac{-b-\lambda_{jk,R}}{\sigma_n}) > Q(\frac{b-\lambda_{jk,R}}{\sigma_n}). \tag{31}$$

Similarly,

$$\varphi(\frac{-b-\lambda_{jk,R}}{\sigma_n}) > \varphi(\frac{b-\lambda_{jk,R}}{\sigma_n}). \tag{32}$$

Due to $\varphi(x) \le Q(x)$, (29) can be reduce to

$$\xi[M]^2 > \frac{1}{k+1}\sum_{j=0}^{k}\frac{(\sigma_n-\lambda_{jk,R})^2}{\sqrt{2\pi}}\exp(-(\frac{b-\lambda_{jk,R}}{\sqrt{2}\sigma_n})^2). \tag{33}$$

Considering that

$$(\lambda_{jk,R})_{\max} = (1+k-(2j-k)\alpha)_{\max} = 1+k\alpha+k, \tag{34}$$

(33) can be rewritten as

$$\xi[M]^2 > \frac{1}{k+1}\sum_{j=0}^{k}\frac{(\sigma_n-\lambda_{jk,R})^2}{\sqrt{2\pi}}\exp(-\frac{b^2k^2\alpha^2}{2\sigma_n^2}) \times \exp(-\frac{b^2[(1+k)^2+2k(1+k)]}{2\sigma_n^2}). \quad (35)$$

Using Cauchy–Schwarz–Buniakowsky inequality [23],

$$(\sum_{k=1}^{n}a_kb_k)^2 \le \sum_{k=1}^{n}a_k^2\sum_{k=1}^{n}b_k^2. \quad (36)$$

Let $b_k = 1$; then, we obtain

$$(\sum_{k=1}^{n}a_k)^2 \le n\sum_{k=1}^{n}a_k^2, \quad (37)$$

and (35) can be reduced to

$$\xi[M] > \frac{1}{(k+1)}\exp(-\frac{b^2[(1+k)^2+2k(1+k)]}{4\sigma_n^2}) \times \exp(-\frac{b^2k^2\alpha^2}{4\sigma_n^2})(\sum_{j=0}^{k}\frac{(\sigma_n+bk)}{(2\pi)^{1/4}} + \sum_{j=0}^{k}\frac{(-(2j-k)bk)}{(2\pi)^{1/4}}). \quad (38)$$

Since

$$\sum_{j=0}^{k}\frac{-(2j-k)bk}{(2\pi)^{1/4}} = 0, \quad (39)$$

we can get

$$\xi[M] > \frac{\sigma_n+bk}{(2\pi)^{1/4}}\exp(-\frac{b^2[(1+k)^2+2k(1+k)]+b^2k^2\alpha^2}{4\sigma_n^2}). \quad (40)$$

ACKNOWLEDGMENT

The authors would like to thank Dr. Gengfa Fang and Dr. Derong Du for their valuable inputs.

REFERENCES

[1] M. N. Tehrani, M. Uysal, and H. Yanikomeroglu, "Device-to-device communication in 5G cellular networks: Challenges, solutions, and future directions," *IEEE Commun. Mag.*, vol. 52, no. 5, pp. 86–92, May 2014.
[2] C. B. Chae, A. Forenza, R. W. Heath, Jr., M. R. McKay, and I. B. Collings, "Adaptive MIMO transmission techniques for broadband wireless communication systems," *IEEE Commun. Mag.*, vol. 48, no. 5, pp. 112–118, May 2010.
[3] D. Marabissi, D. Tarchi, F. Genovese, and R. Fantacci, "Adaptive modulation in wireless OFDMA systems with finite state modeling," in *Proc. IEEE Global Telecommun. Conf.*, Nov. 2007, pp. 5210–5214.
[4] M. D. Yacoub, "The $\kappa-\mu$ distribution and the $\eta-\mu$ distribution," *IEEE Antennas Propag. Mag.*, vol. 49, pp. 68–81, 2007.
[5] J. Medbo, K. Borner, K. Haneda, and V. Hovinen, T. Imai, J. Järvelainen, T. Jämsä, A. Karttunen, K. Kusume, J. Kyröläinen, P. Kyösti, J. Meinilä, V. Nurmela, L. Raschkowski, A. Roivainen, and J. Ylitalo, "Channel modelling for the fifth generation mobile communications," in *Proc. 8th Eur. Conf. Antennas Propag.*, Apr. 2014, pp. 219–223.
[6] D. B. da Costa and M. D. Yacoub, "The $\eta-\mu$ joint phase-envelope distribution," in *Proc. IEEE Wireless Commun. Netw. Conf.*, Mar. 2007, pp. 1906–1908.
[7] I. S. Ansari, F. Yilmaz, and M.-S. Alouini, "On the sum of squared $\eta-\mu$ random variates with application to the performance of wireless communication systems," in *Proc. IEEE 77th Veh. Technol. Conf. (VTC Spring)*, Jun. 2013, pp. 1–6.
[8] L. Hanzo, S. X. Ng, W. T. Webb, and T. Keller, *Quadrature Amplitude Modulation: From Basics to Adaptive Trellis-Coded, Turbo-Equalised and Space-Time Coded OFDM, CDMA and MC-CDMA Systems*. Hoboken, NJ, USA: Wiley, 2004.
[9] J. G. Proakis, *Digital Communications*. Boston, MA, USA: McGraw-Hill, 2001.
[10] F. Yang, X. Zeng, H. Mao, X. Tan, and D. Du, "A novel adaptive modulation based on nondata-aided error vector magnitude in non-line-of-sight condition of wireless sensor network," *Sensors*, vol. 18, no. 1, p. 229, 2018.
[11] H. A. Mahmoud and H. Arslan, "Error vector magnitude to SNR conversion for nondata-aided receivers," *IEEE Trans. Wireless Commun.*, vol. 8, no. 5, pp. 2694–2704, May 2009.
[12] S. Sen, N. Santhapuri, R. R. Choudhury, and S. Nelakuditi, "AccuRate: Constellation based rate estimation in wireless networks," in *Proc. NSDI*, Apr. 2010, p. 12.
[13] V. A. Thomas, S. Kumar, S. Kalyani, M. El-Hajjar, K. Giridhar, and L. Hanzo, "Error vector magnitude analysis of fading SIMO channels relying on MRC reception," *IEEE Trans. Commun.*, vol. 64, no. 4, pp. 1786–1797, Apr. 2016.
[14] S. Kalyani and R. M. Karthik, "The asymptotic distribution of maxima of independent and identically distributed sums of correlated or non-identical gamma random variables and its applications," *IEEE Trans. Commun.*, vol. 60, no. 9, pp. 2747–2758, Sep. 2012.
[15] H. Exton, *Multiple Hypergeometric Functions and Applications*. New York, NY, USA: Halsted Press, Ellis Horwood, 1976.
[16] H. Stark and J. W. Woods, *Probability, Statistics, and Random Processes for Engineers*. London, U.K.: Pearson, 2012.
[17] S. Chen, Y. Wang, F. Qin, Z. Shen, and S. Sun, "LTE-HI: A new solution to future wireless mobile broadband challenges and requirements," *IEEE Wireless Commun.*, vol. 21, no. 3, pp. 70–78, Jun. 2014.
[18] D. B. Da Costa, J. C. S. S. Filho, M. D. Yacoub, and G. Fraidenraich, "Second-order statistics of $\eta-\mu$ fading channels: Theory and applications," *IEEE Trans. Wireless Commun.*, vol. 7, no. 3, pp. 819–824, Mar. 2008.
[19] A. Goldsmith, *Wireless Communications*. Cambridge, U.K.: Cambridge Univ. Press, 2005.
[20] B. Choi and L. Hanzo, "Optimum mode-switching-assisted constant-power single- and multicarrier adaptive modulation," *IEEE Trans. Veh. Technol.*, vol. 52, no. 3, pp. 536–560, May 2003.
[21] R. A. Shafik, M. S. Rahman, and A. R. Islam, "On the extended relationships among EVM, BER and SNR as performance metrics," in *Proc. Int. Conf. Elect. Comput. Eng.*, Dec. 2006, pp. 408–411.
[22] N. L. Johnson and S. Kotz, *Distributions in Statistics: Continuous Univariate Distributions-1*. Boston, MA, USA: Houghton Mifflin, 1970.
[23] I. S. Gradshteyn and I. M. Ryzhik, *Table of Integrals, Series, and Products*, A. Jeffrey and D. Zwillinger, Eds., 7th ed. New York, NY, USA: Academic, 2007.

FAN YANG received the B.E., M.S., and Ph.D. degrees from Chongqing University, Chongqing, China, in 2006, 2010, and 2018, respectively. He is currently an Associate Professor with the School of Electrical and Electronic Engineering, Chongqing University of Technology, Chongqing. He served many Telecom Companies and Institutes in China. From 2010 to 2011, he was an Assistant Engineer with the No. 30 Institute of China Electronic Technology Group Corporation (CETC), Chengdu, China. From 2011 to 2018, he was a Senior Engineer with China Aerospace Science and Industry Corporation (CASIC) and Chongqing Jinmei Communication Company Ltd., Chongqing. His research interests include adaptive transmission in wireless communication systems, mobile broadband wireless networks, and the next generation mobile communication.

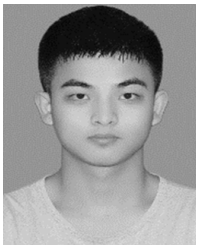

HAIWEI MAO received the B.E. degree in electrical engineering and automation from the University of Electronic Science and Technology, in 2016. He is currently pursuing the M.S. degree with the Department of Electronic and Information Engineering, College of Communication Engineering, Chongqing University, China. His research interest includes wireless broadband adaptive transmission.

XIAOPING ZENG received the B.E., M.S., and Ph.D. degrees in electrical engineering from Chongqing University, Chongqing, China, in 1982, 1987, and 1996, respectively. He is currently a Professor and a Ph.D. Supervisor with the College of Communication Engineering, Chongqing University, China. His research interests include aeronautical information networks, multiple-input–multiple-output systems, and vehicle-to-vehicle communications.

XIN JIAN received the B.E. and Ph.D. degrees from Chongqing University, Chongqing, China, in 2009 and 2014, respectively, where he is currently an Associate Professor with the College of Communication Engineering. His research interests include MIMO systems, vehicle-to-vehicle communications, and the next generation mobile communication.

SHU FU received the Ph.D. degree from the National Key Laboratory of Communications, University of Electronic Science and Technology of China, Chengdu, China. He was a joint Ph.D. Student with the University of Waterloo, from 2014 to 2015. He is currently a Lecturer with the College of Communication Engineering, Chongqing University, Chongqing, China. His research interests include wireless communication and cross networks energy efficiency.

BIN WU (S'04–M'07) received the Ph.D. degree in electrical and electronic engineering from The University of Hong Kong, Hong Kong, in 2007. He was a Postdoctoral Research Fellow with the ECE Department, University of Waterloo, Waterloo, Canada, from 2007 to 2012. He is currently a Professor with the School of Computer Science and Technology, Tianjin University, Tianjin, China. His research interests include computer systems and networking, and communication system design.

XIAOHENG TAN received the B.S. degree in radio communication engineering and the Ph.D. degree in communication engineering from Chongqing University, Chongqing, in 1998 and 2003, respectively, where he is currently a Professor with the College of Communication Engineering. His research interests include modern communication technology and systems, broadband wireless access technology, and adaptive signal processing.

JIHUA ZHOU received the Ph.D. degree from the Institute of Computing Technology, Chinese Academy of Sciences, China, in 2008. He is currently a Vice Chief Engineer with the China Aerospace Science and Industry Corporation (CASIC) and Chongqing Jinmei Communication Company Ltd., Chongqing, China. His research interest includes broadband wireless communication systems design and implementation.